# Pharmacologic Stabilization of Retromer Rescues Endosomal Pathology Induced by Defects in the Alzheimer's gene *SORL1*

Swati Mishra[1,2,4], Allison Knupp[1,2,4,] Chizuru Kinoshita[1,2], Refugio Martinez[1,2], Panos Theofilas[3], and Jessica E. Young[1,2,*]

[1]Department of Laboratory Medicine and Pathology, University of Washington Seattle WA, 98195, USA

[2]Institute for Stem Cell and Regenerative Medicine, University of Washington Seattle WA, 98195, USA

[3]Memory and Aging Center, Department of Neurology, University of California, San Francisco, San Francisco, CA 94158

[4]These authors contributed equally

*Correspondence: jeyoung@uw.edu

## SUMMARY

The Sortilin-related receptor 1 gene (*SORL1,* SORLA) is strongly associated with risk of developing Alzheimer's disease (AD). SORLA is a regulator of endosomal trafficking in neurons and interacts with retromer, a complex that is a 'master conductor' of endosomal trafficking. Pharmacological chaperones stabilize retromer *in vitro*, enhancing its function. Here we used an isogenic series of hiPSC lines with either one or two copies of *SORL1* or harboring one copy of a variant linked to increased risk for AD. We treated hiPSC-derived cortical neurons with the established retromer chaperone, TPT-260, and tested whether indicators of AD's defining endosomal, amyloid, and Tau pathologies were corrected. We observed that the degree of rescue by TPT-260 treatment varied, depending on whether the neurons harbor at least one functional copy of *SORL1* or whether they are fully deficient. Using a disease-relevant preclinical model, our work illuminates how the *SORL1*-retromer pathway can be therapeutically harnessed.

**Introduction:**

Alzheimer's disease (AD) is a devastating neurodegenerative disorder with only a very few medications that alleviate symptoms and no treatment that effectively modifies the course of the disorder for more than several months. Most AD drugs target amyloid beta (Aβ), the main component of senile plaques, which are a hallmark AD neuropathology. However, genetic studies, including large genome-wide association studies, have identified dozens of AD risk loci that map to various cellular processes including endo-lysosomal trafficking(Karch and Goate, 2015). Abnormal endosomes and lysosomes in human brains have long been identified as a pathologic hallmark of Alzheimer's disease(Cataldo et al., 1996; Cataldo et al., 2004; Cataldo et al., 2000). More recent cell biological studies have particularly implicated AD-related deficiencies in trafficking and recycling related to the multi-protein complex retromer, a 'master conductor' of endosomal trafficking (Knupp et al., 2020; Simoes et al., 2021; Young et al., 2018). Central to this mechanism is the gene *SORL1*, an endosomal sorting receptor that has emerged as a highly pathogenic AD gene(Scheltens et al., 2021). Missense variants or frameshift variants leading to premature stop codons in *SORL1* can contribute to AD pathogenesis through loss of function of *SORL1(*Pottier et al., 2012; Vardarajan et al., 2014). The *SORL1* gene encodes the sorting receptor SORLA, which engages with the multi-protein sorting complex retromer as an adaptor protein for multiple cargo, including APP, neurotrophin receptors, and glutamate receptors(Fjorback et al., 2012; Mishra et al., 2022; Simoes et al., 2021). *SORL1* KO neurons derived from hiPSCs have endosomal traffic jams, mislocalized neuronal cargo and show impairments in endosomal degradation and recycling(Hung et al., 2021; Knupp et al., 2020; Mishra et al., 2022). Both endosomal recycling and degradation pathways in neurons are enhanced in a model where *SORL1* is overexpressed(Mishra et al., 2022), suggesting that increasing *SORL1* expression in neurons may be beneficial in AD. However, *SORL1* is a difficult therapeutic target due to its size: the gene contains 48 exons and large intronic regions and the protein itself is 2214 amino acids(Rogaeva et al., 2007).

Enhancing endosomal trafficking via targeting the retromer complex, which is intimately associated with *SORL1*, may be a feasible therapeutic strategy. Small molecule pharmacologic chaperones that stabilize the cargo recognition core of retromer have been developed and reduce amyloidogenic processing of APP in a mouse model of AD and increase the flow of SORLA through endosomes(Mecozzi et al., 2014). Retromer chaperones have been shown to reduce Aβ and phospho-Tau in hiPSC-cortical neurons from AD and controls and promote neuroprotection in hiPSC-motor neurons from amyotrophic lateral sclerosis (ALS) patients (Muzio et al., 2020; Young et al., 2018). However, how they affect other defining pathologies of AD (ie: endosomal pathologies) has not been shown.

We used our previously published *SORL1* deficient hiPSC cell lines (*SORL1* KO)(Knupp et al., 2020) and new lines engineered to have loss of *SORL1* on one allele ($SORL1^{+/-}$) or to have one copy of an AD-associated *SORL1* variant ($SORL1^{Var}$) to investigate whether enhancing retromer-related trafficking using TPT-260, an established retromer chaperone(Chu and Pratico, 2017; Mecozzi et al., 2014; Vagnozzi et al., 2021), can improve endosomal phenotypes. We report that in neurons derived from $SORL1^{+/-}$ and $SORL1^{Var}$ lines, we observe enlarged early endosomes and increased Aβ secretion. We show that treatment with TPT-260, rescues these phenotypes. We also report than TPT-260 can improve endo-lysosomal trafficking and endosomal recycling in *SORL1* deficient hiPSC-derived neurons. In addition to rescuing endo-lysosomal phenotypes, TPT-260 lowers Aβ and phosphorylated Tau (p-Tau), suggesting that this pathway can converge on multiple cellular phenotypes in AD. Importantly, for some of the phenotypes we studied having one functional copy of *SORL1* ($SORL1^{+/-}$) provided a more complete rescue than in neurons fully deficient in *SORL1* (*SORL1* KO). As loss of one copy of *SORL1* has been shown to be causative for AD our data suggest that the *SORL1*-retromer axis is important for future therapeutic development in AD.

**Results:**

***SORL1*$^{+/-}$ and *SORL1*$^{Var}$ hiPSC-derived neurons have swollen early endosomes and increased Aβ secretion.**

Variants in the VPS10 domain of *SORL1* have been shown to be damaging(Holstege et al., 2017). Using CRISPR/Cas9 genome editing, we generated isogenic stem cell lines containing either heterozygous AD-associated variants in the VPS10 domain: E270K, Y141C, and G511R *(SORL1*$^{Var}$) or heterozygous *SORL1* knockout line (*SORL1*$^{+/-}$) **(Figure S1).** These variants have all been associated with increased AD risk(Caglayan et al., 2014; Pottier et al., 2012; Vardarajan et al., 2014). Western blot analysis revealed that *SORL1*$^{Var}$ neurons do not have a loss of SORLA protein expression as these missense variants do not introduce a frame-shift **(Figure S1**) or destabilize the protein enough for it to be degraded. However, *SORL1*$^{+/-}$ neurons have 50% of *SORL1* expression compared with isogenic WT controls (**Figure S1).**

We and others have previously observed enlarged early endosomes in homozygous *SORL1* KO hiPSC-derived neurons(Hung et al., 2021; Knupp et al., 2020). We hypothesized that *SORL1*$^{+/-}$ and *SORL1*$^{Var}$ neurons would similarly contain enlarged early endosomes, although we predicted that due to the single copy of WT *SORL1*, the phenotype could be more subtle. We immunostained *SORL1* KO, *SORL1*$^{+/-}$, and *SORL1*$^{Var}$ neurons with EEA1 to mark early endosomes, imaged cells using confocal microscopy, and quantified early endosome size using Cell Profiler as we have previously described(Knupp et al., 2020). We observed a significant increase in endosome size in *SORL1*$^{Var}$, *SORL1*$^{+/-}$, and *SORL1* KO neurons compared to isogenic WT controls (**Figure 1 A-B**). Interestingly, endosomes in neurons with one copy of WT *SORL1* (*SORL1*$^{Var}$ and *SORL1*$^{+/-}$) were not as enlarged as in cells fully deficient in *SORL1* (*SORL1* KO) (**Figure 1B**).

When SORLA is absent, APP is stuck in early and recycling endosomes where it can be more readily processed to Aβ(Das et al., 2016; Knupp et al., 2020; Mishra et al., 2022; Tan and

Gleeson, 2019; Toh et al., 2018). We have previously reported increased secreted Aβ in *SORL1* KO neurons(Knupp et al., 2020) and here we observed an increase in secreted Aβ peptides in *SORL1*$^{+/-}$ or *SORL1*$^{Var}$ neurons compared to WT neurons. Consistent with having one functional copy of *SORL1*, the increase in Aβ was not as pronounced as with the full *SORL1* KO (**Figure 1C-D**).

**TPT-260 treatment reduces endosome size, secreted Aβ levels and pTau levels in *SORL1* KO, *SORL1*$^{+/-}$, and *SORL1*$^{Var}$ neurons.**

We next tested whether enhancing endo-lysosomal function via small molecules could rescue pathological phenotypes. We chose to study the effects of a pharmacological chaperone, TPT-260 (also called R55), which stabilizes and enhances retromer by binding the VPS35-VPS26-VPS29 trimer in the cargo-recognition core of the multi-subunit retromer complex(Mecozzi et al., 2014). Previously, we have shown that a similar molecule, TPT-172 (also known as R33), was effective at reducing Aβ and pTau levels in hiPSC-derived neurons from AD patients and controls(Young et al., 2018). First, we tested whether TPT-260 treatment would influence early endosome size. In *SORL1* KO, *SORL1*$^{+/-}$, and *SORL1*$^{Var}$ neurons, treatment with TPT-260 reduced endosome size compared with vehicle (DMSO) treated controls (**Figure 2A-B**). In TPT-260 treated *SORL1*$^{+/-}$ and *SORL1*$^{Var}$ neurons, endosome size was not significantly different than in WT neurons treated with TPT-260. However, while endosome size was also reduced in neurons with full *SORL1* KO, it was not reduced to WT levels, indicating that without at least one copy of *SORL1*, this phenotype cannot be fully resolved (**Figure 2B**). We did not observe any changes in EEA1 puncta size in WT neurons treated with TPT260, indicating that the retromer chaperone does not alter the size of endosomes that are not enlarged.

We next tested whether TPT-260 treatment could reduce Aβ peptides in *SORL1* KO, *SORL1*$^{+/-}$ or *SORL1*$^{Var}$ neurons. From TPT-treated cultures we measured the amount of Aβ

peptides secreted into the media using an ELISA assay. In all cell lines we observed decreased secreted Aβ peptides, however in neurons with full *SORL1* KO Aβ 1-40 levels, while reduced, were still significantly higher than in the other conditions **(Figure 2C)**. Interestingly, Aβ 1-42 levels were not changed in *SORL1* KO neurons although they were reduced to WT levels in all cell lines with one copy of *SORL1* (**Figure 2D).**

Accumulation of phosphorylated Tau (pTau) protein is a significant neuropathological hallmark in AD and retromer chaperones have been reported to decrease pTau levels in both hiPSC-neurons and mouse models of AD and tauopathy(Li et al., 2020; Young et al., 2018). In our hiPSC-neuronal model, we did not detect significant changes in pTau in neurons without *SORL1* or in any of our *SORL1*$^{Var}$ neurons (**Figure S2**), although in other studies where *SORL1* KO hiPSC-derived neurons are differentiated using the expression of the transcription factor NGN2, loss of *SORL1* does lead to increased phospho-Tau (Tracy Young-Pearse, personal communication). Despite this, when we treated all genotypes of neurons with TPT-260, we observed that treatment did significantly reduce pTau at several epitopes and there was no difference in the level of reduction relative to whether neurons were fully deficient in *SORL1* or harbored an AD risk variant (**Figure 2 E-G**).

**TPT-260 treatment fully reduces localization of VPS35 from early endosomes, but only partially rescues localization of APP from early endosomes in *SORL1* KO neurons.**

In *SORL1* KO neurons, both VPS35, a core component of retromer, and APP have increased localization in early endosomes(Knupp et al., 2020; Mishra et al., 2022). We examined whether TPT-260 treatment could correct this mis-localization. By performing colocalization analysis for EEA1 (early endosomes) and VPS35, we observed that *SORL1*$^{+/-}$ neurons also had increased VPS35 accumulation in early endosomes (**Figure 3A-B**). Treatment with TPT-260 completely rescued VPS35/EEA1 colocalization in *SORL1*$^{+/-}$ and *SORL1* KO neurons, indicating that this

treatment was able to mobilize retromer away from early endosomes (**Figure 3A-B**). *SORL1*$^{+/-}$ neurons also have increased colocalization of APP with EEA1, however upon TPT-260 treatment APP/EEA1 colocalization was completely resolved in *SORL1*$^{+/-}$ neurons, while there was still significantly more APP in early endosomes in treated *SORL1* KO neurons. (**Figure 3C-D**). This observation is consistent with *SORL1* being a main adaptor protein for APP and retromer via VPS26(Fjorback et al., 2012) and could explain why the reduction of Aβ peptides in TPT-260 treated *SORL1* KO neurons is not as significant as in neurons with at least one WT copy of *SORL1*; in neurons without any copies of *SORL1*, APP is still largely localized to early endosomes where it can be processed to Aβ.

**Impaired endosomal recycling and lysosomal degradation in *SORL1* KO neurons are improved by pharmacologic stabilization of retromer**

In *SORL1* KO neurons, endosomal traffic jams impede cargo traffic to late endosomes and lysosomes as well as to the cell surface recycling pathway(Mishra et al., 2022). The latter function has been shown to involve a neuron-specific subunit of retromer, VPS26b(Simoes et al., 2021). We analyzed lysosomal degradation in WT and *SORL1* KO neurons treated with TPT-260 or vehicle (DMSO) using the DQ-Red-BSA assay(Marwaha and Sharma, 2017). We observed a significant reduction in DQ-Red-BSA fluorescence, indicating impaired degradation, at 24 hours in DMSO treated *SORL1* KO neurons (**Figure 4B**), consistent with our previous observations(Mishra et al., 2022). In TPT-260 treated neurons, we document a complete rescue of this phenotype (**Figure 4B**) suggesting that retromer stabilization can promote this pathway, even in the absence of *SORL1*.

To test endosomal recycling, we utilized the transferrin recycling assay, a measure of both fast and slow endosomal recycling(Ouellette and Carabeo, 2010; Sonnichsen et al., 2000).

We found that in *SORL1* KO neurons, TPT-260 treatment only partially rescued endosomal recycling (**Figure 4 C-D**). However, when TPT-260 treated *SORL1*$^{+/-}$ neurons were analyzed, we document a complete rescue of transferrin recycling (**Figure 4 C,E**). These data suggest that enhancing retromer can promote endosomal recycling but at least one functional copy of *SORL1* is needed to recycle cargo as efficiently as in WT neurons.

## Discussion

When considering the development of novel therapeutics for Alzheimer's disease, it is critical to examine biologically relevant pathways such as protein trafficking through the endo-lysosomal network. In particular, trafficking of APP directly affects its processing into Aβ. Furthermore, indicators of endosomal dysfunction are early cytopathological phenotypes in AD, evident before substantial accumulation of other neuropathologic hallmarks(Cataldo et al., 2000) and thus a potentially attractive early therapeutic readout. In order to more fully explore this concept in human neurons, we used previously published and newly generated hiPSC lines that are either deficient in *SORL1* expression (*SORL1* KO or *SORL1*$^{+/-}$) or that harbor AD-associated coding variants in the VPS10 domain of the protein (*SORL1*$^{Var}$) and treated neurons differentiated from these hiPSCs with TPT-260, a small molecule chaperone that stabilized retromer and enhances its function(Mecozzi et al., 2014).

We and others have previously reported that heterozygous and homozygous loss of *SORL1* results in increased secretion of Aβ and enlarged early endosomes(Hung et al., 2021; Knupp et al., 2020). In this study, we also observed increases in secreted Aβ and enlarged endosomes in our *SORL1*$^{Var}$ lines (**Figure 1**). Both secreted Aβ and enlarged early endosome phenotypes seem to be dependent on whether a WT allele of *SORL1* is present, which aligns with previous reports(Dodson et al., 2008; Hung et al., 2021). These data are also consistent with indications that *SORL1* haploinsufficiency is causative for AD(Holstege et al., 2017; Scheltens et

al., 2021), and suggests that certain AD-associated variants may result in loss of important *SORL1* functions.

SORLA, is the main adaptor protein for retromer-dependent trafficking of APP and Aβ peptides(Andersen et al., 2005; Caglayan et al., 2014; Fjorback et al., 2012). Therefore, in *SORL1* KO neurons, there is a smaller effect on Aβ secretion after treatment with TPT-260 (**Figure 2).** However, in the more clinically relevant scenario of either *SORL1*$^{+/-}$or *SORL1*$^{Var}$, TPT-260 treatment reduced both Aβ40 and Aβ42 to WT levels.

TPT260 treatment lowers phospho-Tau levels on multiple epitopes in this model, highlighting the potential therapeutic relevance of retromer functional enhancement. Our data here (**Figure 2**) provide an independent corroboration of previous work(Young et al., 2018)and also supports what has been seen in tauopathy models(Li et al., 2020; Young et al., 2018). Tau clearance by endo-lysosomal trafficking is an important aspect of maintaining Tau homeostasis and efficient clearance of phosphorylated Tau is an important step in preventing pathological aggregation(Tang et al., 2019).

Our data provides the first evidence that a small molecule can correct early endosome enlargement. TPT-260 treatment reduced endosome size in all genotypes, however only in neurons with at least one copy of *SORL1* were endosome sizes fully reduced to WT levels (**Figure 2**). Importantly for therapeutic implications, the retromer chaperone does not appear to affect endosome size in the WT cell lines at the concentrations we tested.

APP and VPS35 are both increased in early endosomes in *SORL1* KO neurons(Knupp et al., 2020; Mishra et al., 2022). TPT-260 treatment reduced the localization of VPS35 in early endosomes to WT levels in *SORL1* KO cells, showing that this treatment is sufficient to mobilize retromer in these cells (**Figure 3**). However, because SORLA is a main adaptor protein between retromer and APP, in full *SORL1* KO cells, there is not a large change in APP localization with TPT-260 treatment (**Figure 3**). In neurons with at least one copy of *SORL1* (*SORL1*$^{+/-}$) neurons,

TPT-260 treatment APP co-localization with early endosomes is similar to WT APP/EEA1 co-localization (**Figure 3**). A large part of amyloidogenic cleavage of APP occurs in the early endosomes, so this finding could explain why Aβ levels in *SORL1*$^{+/-}$ neurons are completely rescued with TPT-260 treatment, while Aβ levels in *SORL1* KO neurons are not.

Endosomal traffic jams impact multiple arms of the endo-lysosomal network. Using a DQ-Red-BSA assay, we observe that TPT-260 enhances lysosomal degradation in *SORL1* KO cells, bringing this function to WT levels (**Figure 4**). On the other hand, we observed only a partial rescue of transferrin recycling in *SORL1* KO cells but a full rescue in *SORL1*$^{+/-}$ neurons (**Figure 4**). In neurons, *SORL1* interacts with a neuron-specific isoform of the retromer complex, VPS26b, to recycle cargo such as glutamate receptors(Simoes et al., 2021). Our data suggest that in *SORL1* KO, retromer enhancement is not enough to fully rescue this phenotype but would be beneficial in *SORL1*$^{+/-}$ cells.

Our work shows that treatment with a small molecule that stabilizes retromer in *vitro* and enhances retromer-related trafficking can reduce important cellular and neuropathologic phenotypes in human AD neuronal models. Using TPT-260, we broadly show that enhancement of retromer-related trafficking can fully or partially rescue deficits induced by loss of *SORL1*. Although there is one report of a full loss of *SORL1*(Le Guennec et al., 2018), most patients where *SORL1* is a main risk factor for disease development still maintain at least one functional copy of *SORL1*. Our work provides evidence that the *SORL1*-retromer pathway is a strong candidate for therapeutic intervention in AD. This study builds on previous work that has used these chaperones in animals and human cells, suggesting that studies such as this could represent an important pre-clinical step in identifying new therapeutic molecules for AD.

**Limitations to our study:** Our study has certain limitations. First, we focused on variants present in the VPS10 domain of *SORL1*(Andersen et al., 2016; Pottier et al., 2012; Vardarajan et al.,

2014). Some of these variants have been found in control subjects(Holstege et al., 2017), thus there are other factors in various human genetic backgrounds that need to be considered. We engineered these variants in our well-characterized, male, hiPSC line(Knupp et al., 2020; Young et al., 2015). The genetic background of this line also harbors one copy of APOE ε4 and common variants in *SORL1* associated with increased AD risk in candidate-gene based studies(Levy et al., 2007; Rogaeva et al., 2007). We cannot rule out the contribution of these other genomic variants to our phenotypes; however rescue of these cellular phenotypes using retromer-enhancing drugs is still an important observation that may be relevant to both earlier and later-onset forms of AD. Finally, our study is focused on neuronal cells. We recognize the importance of endosomal trafficking and *SORL1*-retromer related pathways in glia and other cell types relevant to the pathogenesis and/or progression of AD. Future studies will benefit from analyzing endo-lysosomal phenotypes in multiple CNS cell types.

Experimental procedures

**Cell lines**

**CRISPR/Cas9 Genome Editing**

All genome editing was completed in the previously published and characterized CV background human induced pluripotent stem cell line (Young et al., 2015), which is male with an APOE e3/e4 genotype(Levy et al., 2007). Genome editing was performed according to published protocols (Young et al., 2018)(Knupp et al., 2020). Further details about gene editing are described in the supplemental methods.

**Neuronal Differentiation**

hiPSCs were cultured and differentiated into neurons using dual SMAD inhibition protocols(Shi et al., 2012), modified previously in our laboratory (Knupp et al., 2020; Mishra et al., 2022; Rose et al., 2018). Further details about the neuronal differentiations are described in the supplemental methods.

**Purification of hiPSC-derived neurons**

hiPSC-derived neurons were purified using magnetic bead sorting. Details of the procedure are described in the supplemental methods.

**DQ-Red BSA assay**

Lysosomal proteolytic degradation was evaluated using DQ Red BSA (#D-12051; Thermo Fisher Scientific) following published protocols(Davis et al., 2021; Marwaha and Sharma, 2017; Mishra et al., 2022). More details are described in the supplemental methods.

**Immunocytochemistry**

Details of immunocytochemistry and antibodies used are described in the supplemental procedures.

**Confocal microscopy, Image processing and colocalization analysis.**

All microscopy and image processing were performed under blinded conditions. Confocal z stacks were obtained using a Nikon A1R confocal microscope with x63 and x100 plan apochromat oil immersion objectives or a Nikon Yokogawa W1 spinning disk confocal microscope and a 100X plan apochromat oil immersion objective. Image processing was performed using ImageJ software (Schindelin et al., 2012). For endosome analysis, 10-20 fields were analyzed for a total of 10-58 cells. To investigate colocalization of APP and VPS35 with early endosomes, hiPSC-derived neurons were co-labeled with either APP or VPS35 and early endosome marker EEA1. A minimum of 10 fields of confocal were captured. Median filtering was used to remove noise from images and Otsu thresholding was applied to all images. Colocalization was quantified using the JACOP plugin in Image J software and presented as Mander's correlation co-efficient. More details can be found in the supplemental methods.

**Transferrin recycling assay**

To measure recycling pathway function, we utilized transferrin recycling assay as previously described (Sakane et al., 2014)(Mishra et al., 2022). More details are described in the supplemental methods.

**Western Blotting**

Details of western blotting used in this study are described in the supplemental methods.

**Measurement of secreted Amyloid Beta 1-40 and 1-42**

Aβ peptides were measured using an MSD Aβ V-PLEX assay (Meso Scale Discovery #151200E-2) following manufacturers protocols.

**Measurement of phosphorylated and total tau by ELISA**

Phosphorylated tau protein were measured using a Phospho(Thr231)/Total Tau ELISA plate ( # K15121D-2; Meso Scale Discovery) following manufacturers protocols.

**Quantification and statistical analysis**

The data here represent, when possible, multiple hiPSC clones. This includes two or three WT clones, two *SORL1*KO clones and one *SORL1*$^{+/-}$ clone. Only one *SORL1*$^{+/-}$ clone was recovered during the gene-editing process. For the *SORL1*$^{Var}$ lines and experiments we analyzed two E270K clones, two G511R clones, and one Y141C clone. Only one Y141C clone was recovered during the gene-editing process. All data represents three independent experiments per clone. Experimental data was tested for normal distributions using the Shapiro-Wilk normality test. Normally distributed data was analyzed using parametric two-tailed unpaired t tests, one-way ANOVA tests, or two-way ANOVA tests. Significance was defined as a value of $p > 0.05$. All statistical analysis was completed using GraphPad Prism software. Further details of quantification and statistical analysis for all experiments are provided in the supplemental procedures.

**Acknowledgments**

This work was supported by NIH grant R01AG062148, a BrightFocus Foundation grant (A2018656S), the WeillNeuroHub and Sponsored Research Agreements from Biogen and Retromer Therapeutics to J.E.Y. A.K. was supported by a NIH training grant (T32 AG052354). S.M is supported by a UW ADRC Development grant. Further support for this work comes from a generous gift from the Ellison Foundation (to UW). We thank all the members of the Young

Laboratory as well as Dr. Scott A. Small and Dr. Gregory A. Petsko for critical comments, discussions and feedback on this work. We would like to acknowledge the UW SLU Cell Analysis Facility and the Garvey Imaging Core at the UW Institute for Stem Cell and Regenerative Medicine.

## Author Contributions

Conceptualization: J.E.Y, A.K., S.M. Experimental Design: J.E.Y., A.K, and S.M. Experimental performance: A.K., S.M, R.M, C.K, P.T. Writing-Original draft: A.K. and J.E.Y. Writing-Reviewing and editing: S.M., A.K. and J.E.Y. Funding acquisition: J.E.Y, A.K, and S.M. Supervision: J.E.Y. All authors read and approved the final manuscript.

## FIGURE LEGENDS

Figure 1. ***SORL1*$^{+/-}$ and *SORL1*$^{Var}$ hiPSC-derived neurons have swollen early endosomes and increased Aβ secretion (A)** Representative immunofluorescent images of WT, heterozygous *SORL1*$^{Var}$, *SORL1*$^{+/-}$, and *SORL1* KO hiPSC-derived neurons. Scale bar: 5 μm. **(B)** The size of EEA1 puncta is larger in *SORL1*$^{Var}$, *SORL1*$^{+/-}$, and *SORL1* KO neurons than in WT neurons, indicated by asterisks. The difference between *SORL1* KO, *SORL1*$^{+/-}$, and *SORL1*$^{Var}$ is indicated by hashmarks. **(C-D)** Heterozygous *SORL1*$^{Var}$, *SORL1*$^{+/-,}$ and *SORL1* KO hiPSC-derived neurons secrete increased levels of **(C)**$A\beta_{40}$ and **(D)**$A\beta_{42}$ as compared to WT controls (asterisks). *SORL1* KO neurons secrete increased levels of $A\beta_{40}$ and $A\beta_{42}$ as compared to *SORL1*$^{Var}$ and *SORL1*$^{+/-}$ hiPSC-derived neurons. (hashmarks)**.** For imaging experiments, 10-15 images and 1-3 clones per genotype were analyzed per genotype. For Aβ secretion experiments, 1-3 clones per genotype and 3 independent experiments per clone per genotype were used. Data represented as mean ± SD. Data was analyzed using parametric one-way ANOVA. Significance was defined as a value of *p < 0.05, **p < 0.01, ***p < 0.001, and ****p < 0.0001.

Figure 2**. Retromer enhancement with TPT-260 reduces AD pathological phenotypes**

Representative immunofluorescent images of TPT-260 and DMSO-treated WT, heterozygous *SORL1*$^{Var}$, *SORL1*$^{+/-}$ and *SORL1* KO hiPSC-derived neurons. Scale bar: 5 µm. **(B)** TPT-260 treatment reduces endosome size in *SORL1*$^{Var}$, *SORL1*$^{+/-}$, and *SORL1* KO neurons (indicated by asterisks). Endosome size in TPT-260 treated *SORL1* KO neurons is significantly different from *SORL1*$^{Var}$ and *SORL1*$^{+/-}$ neurons (indicated by hashmarks). N=10-20 images analyzed per genotype. Data represented as mean ± SD. **(C-D)** Levels of secreted Aβ 1-40 **(C)** and Aβ 1-42 **(D)** are reduced with TPT-260 treatment in all genotypes, compared to DMSO, except secreted Aβ 1-42 in *SORL1* KO neurons (indicated by asterisks). The % decrease in Aβ 1-40 and Aβ 1-42 levels of TPT-260 treated cells is greater in *SORL1*$^{Var}$ and *SORL1*$^{+/-}$ neurons as compared to *SORL1* KO neurons (indicated by hashmarks). For all experiments, 1-3 clones per genotype and 3 independent experiments per clone per genotype were used. Data represented as mean ±SD. (**E-G**) Tau phosphorylation on three epitopes was examined in response to TPT-260 treatment. **(E)** Thr 231 epitope levels, as measured by ELISA assay, is reduced in all the genotypes treated with TPT-260 relative to WT DMSO controls **(F)** The PHF-1 (Ser396/Ser404) and the **(G)** AT8(Ser202/Thr305) epitopes as measured by western blot is decreased in TPT-260 treated *SORL1* KO hiPSC-derived neurons relative to WT DMSO controls. 1-3 clones were analyzed per genotype. For all experiments, 1-3 clones per genotype and 3 independent experiments per clone per genotype were used. Data represented as mean ± SD. Normally distributed data was analyzed using parametric two-way ANOVA. 1-3 clones were analyzed per genotype. Significance was defined as a value of *p < 0.05, **p < 0.01, ***p < 0.001, and ****p < 0.0001. ns=not significant.

Figure 3. **TPT-260 treatment reduces localization of APP and VPS35 in early endosomes.** **(A-B)** Co-localization of VPS35 (green) with EEA1 (red) is increased in *SORL1*$^{+/-}$ and *SORL1* KO neurons and TPT-260 reduces co-localization (asterisks). In *SORL1*$^{+/-}$ and *SORL1* KO neurons,

treatment with TPT-260 colocalization of VPS35 and EEA1 is not different than in WT cells (white arrows, ns). **(C-D)** Co-localization of APP (green) with EEA1 (red) co-localization is increased in *SORL1*$^{+/-}$ and *SORL1* KO neurons and TPT-260 reduces co-localization (asterisks). Treatment with TPT-260 reduces APP/EEA1 colocalization to a greater extent in *SORL1* $^{+/-}$ neurons such that it is not different from WT neurons treated with TPT-260 (white arrows, ns). However, in *SORL1* KO neurons, APP/EEA1 colocalization is still significantly increased compared to WT cells (white arrows, asterisks). Scale bar: 5μm. For co-localization analysis, 10-15 images per clones and 1-2 clones per genotype were analyzed per genotype and 3 independent experiments per clone per genotype were performed. Data represented as mean ± SD. Data was analyzed using parametric one-way ANOVA. Significance was defined as a value of *p < 0.05, **p < 0.01, ***p < 0.001, and ****p < 0.0001.

Figure 4. **Retromer enhancement with TPT-260 enhances lysosomal degradation and endosomal recycling in *SORL1* KO neurons. (A-B)** TPT-260 rescues degradation of DQ-Red BSA. **(A)** Representative images of WT and *SORL1* KO neurons treated with DQ-Red-BSA for 24 hours. **(B)**TPT-260 rescues lysosomal degradation shown by increased fluorescence intensity of DQ-Red BSA after 24 hrs in TPT-260 treated *SORL1* KO neurons as compared DMSO. There is no difference between DMSO treated and TPT-260 treated WT hiPSC-derived neurons. Scale bar: 5 μm. **(C)** Representative images of WT, SORL1$^{+/-}$, and SORL1 KO neurons labeled with fluorescent transferrin. **(D)** TPT-260 only partially rescues endosomal recycling in *SORL1* KO neurons. TPT-260 treated *SORL1* KO neurons (dark orange) do not recycle transferrin as efficiently as WT neurons (black/gray). Asterisks indicate a statistical difference between WT DMSO and *SORL1* KO DMSO neurons. Hashmarks indicate a statistical difference between TPT-260 treated *SORL1* KO and TPT-260 treated WT neurons. **(E)** TPT-260 completely rescues endosomal recycling in *SORL1*$^{+/-}$ neurons (light orange) compared to DMSO (dark orange). There is no difference between TPT-260 treated *SORL1*$^{+/-}$ neurons and TPT-260 WT neurons (gray

lines). Asterisks indicate a statistical difference between WT DMSO and *SORL1*$^{+/-}$ DMSO; NS indicates a non-significant difference between *SORL1*$^{+/-}$ +TPT-260 and WT+TPT-260. Scale bar: 5 µm. Data represented as transferrin intensity normalized to time 0. 10 images per clone per genotype per timepoint were analyzed. 1-2 clones per genotype were analyzed and 3 independent experiments per clone per genotype were performed. Data represented as mean +/- SD. Data represented as mean ± SD. Normally distributed data was analyzed using parametric two-way ANOVA. Significance was defined as a value of *p < 0.05, **p < 0.01, ***p < 0.001, and ****p < 0.0001. ns= not significant.

**References**

Andersen, O.M., Reiche, J., Schmidt, V., Gotthardt, M., Spoelgen, R., Behlke, J., von Arnim, C.A., Breiderhoff, T., Jansen, P., Wu, X*., et al.* (2005). Neuronal sorting protein-related receptor sorLA/LR11 regulates processing of the amyloid precursor protein. Proc Natl Acad Sci U S A *102*, 13461-13466.

Andersen, O.M., Rudolph, I.M., and Willnow, T.E. (2016). Risk factor SORL1: from genetic association to functional validation in Alzheimer's disease. Acta Neuropathol *132*, 653-665.

Caglayan, S., Takagi-Niidome, S., Liao, F., Carlo, A.S., Schmidt, V., Burgert, T., Kitago, Y., Fuchtbauer, E.M., Fuchtbauer, A., Holtzman, D.M*., et al.* (2014). Lysosomal sorting of amyloid-beta by the SORLA receptor is impaired by a familial Alzheimer's disease mutation. Science translational medicine *6*, 223ra220.

Cataldo, A.M., Hamilton, D.J., Barnett, J.L., Paskevich, P.A., and Nixon, R.A. (1996). Properties of the endosomal-lysosomal system in the human central nervous system: disturbances mark most neurons in populations at risk to degenerate in Alzheimer's disease. J Neurosci *16*, 186-199.

Cataldo, A.M., Petanceska, S., Terio, N.B., Peterhoff, C.M., Durham, R., Mercken, M., Mehta, P.D., Buxbaum, J., Haroutunian, V., and Nixon, R.A. (2004). Abeta localization in abnormal endosomes: association with earliest Abeta elevations in AD and Down syndrome. Neurobiol Aging *25*, 1263-1272.

Cataldo, A.M., Peterhoff, C.M., Troncoso, J.C., Gomez-Isla, T., Hyman, B.T., and Nixon, R.A. (2000). Endocytic pathway abnormalities precede amyloid beta deposition in sporadic Alzheimer's disease and Down syndrome: differential effects of APOE genotype and presenilin mutations. Am J Pathol *157*, 277-286.

Chu, J., and Pratico, D. (2017). The retromer complex system in a transgenic mouse model of AD: influence of age. Neurobiol Aging *52*, 32-38.

Das, U., Wang, L., Ganguly, A., Saikia, J.M., Wagner, S.L., Koo, E.H., and Roy, S. (2016). Visualizing APP and BACE-1 approximation in neurons yields insight into the amyloidogenic pathway. Nat Neurosci *19*, 55-64.

Davis, S.E., Roth, J.R., Aljabi, Q., Hakim, A.R., Savell, K.E., Day, J.J., and Arrant, A.E. (2021). Delivering progranulin to neuronal lysosomes protects against excitotoxicity. J Biol Chem *297*, 100993.

Dodson, S.E., Andersen, O.M., Karmali, V., Fritz, J.J., Cheng, D., Peng, J., Levey, A.I., Willnow, T.E., and Lah, J.J. (2008). Loss of LR11/SORLA enhances early pathology in a mouse model of amyloidosis: evidence for a proximal role in Alzheimer's disease. J Neurosci *28*, 12877-12886.

Fjorback, A.W., Seaman, M., Gustafsen, C., Mehmedbasic, A., Gokool, S., Wu, C., Militz, D., Schmidt, V., Madsen, P., Nyengaard, J.R.*, et al.* (2012). Retromer binds the FANSHY sorting motif in SorLA to regulate amyloid precursor protein sorting and processing. J Neurosci *32*, 1467-1480.

Holstege, H., van der Lee, S.J., Hulsman, M., Wong, T.H., van Rooij, J.G., Weiss, M., Louwersheimer, E., Wolters, F.J., Amin, N., Uitterlinden, A.G.*, et al.* (2017). Characterization of pathogenic SORL1 genetic variants for association with Alzheimer's disease: a clinical interpretation strategy. Eur J Hum Genet *25*, 973-981.

Hung, C., Tuck, E., Stubbs, V., van der Lee, S.J., Aalfs, C., van Spaendonk, R., Scheltens, P., Hardy, J., Holstege, H., and Livesey, F.J. (2021). SORL1 deficiency in human excitatory neurons causes APP-dependent defects in the endolysosome-autophagy network. Cell Rep *35*, 109259.

Karch, C.M., and Goate, A.M. (2015). Alzheimer's disease risk genes and mechanisms of disease pathogenesis. Biol Psychiatry *77*, 43-51.

Knupp, A., Mishra, S., Martinez, R., Braggin, J.E., Szabo, M., Kinoshita, C., Hailey, D.W., Small, S.A., Jayadev, S., and Young, J.E. (2020). Depletion of the AD Risk Gene SORL1 Selectively Impairs Neuronal Endosomal Traffic Independent of Amyloidogenic APP Processing. Cell Rep *31*, 107719.

Le Guennec, K., Tubeuf, H., Hannequin, D., Wallon, D., Quenez, O., Rousseau, S., Richard, A.C., Deleuze, J.F., Boland, A., Frebourg, T.*, et al.* (2018). Biallelic Loss of Function of SORL1 in an Early Onset Alzheimer's Disease Patient. J Alzheimers Dis *62*, 821-831.

Levy, S., Sutton, G., Ng, P.C., Feuk, L., Halpern, A.L., Walenz, B.P., Axelrod, N., Huang, J., Kirkness, E.F., Denisov, G.*, et al.* (2007). The diploid genome sequence of an individual human. PLoS Biol *5*, e254.

Li, J.G., Chiu, J., Ramanjulu, M., Blass, B.E., and Pratico, D. (2020). A pharmacological chaperone improves memory by reducing Abeta and tau neuropathology in a mouse model with plaques and tangles. Mol Neurodegener *15*, 1.

Marwaha, R., and Sharma, M. (2017). DQ-Red BSA Trafficking Assay in Cultured Cells to Assess Cargo Delivery to Lysosomes. Bio Protoc *7*.

Mecozzi, V.J., Berman, D.E., Simoes, S., Vetanovetz, C., Awal, M.R., Patel, V.M., Schneider, R.T., Petsko, G.A., Ringe, D., and Small, S.A. (2014). Pharmacological chaperones stabilize retromer to limit APP processing. Nature chemical biology *10*, 443-449.

Mishra, S., Knupp, A., Szabo, M.P., Williams, C.A., Kinoshita, C., Hailey, D.W., Wang, Y., Andersen, O.M., and Young, J.E. (2022). The Alzheimer's gene SORL1 is a regulator of endosomal traffic and recycling in human neurons. Cell Mol Life Sci *79*, 162.

Muzio, L., Sirtori, R., Gornati, D., Eleuteri, S., Fossaghi, A., Brancaccio, D., Manzoni, L., Ottoboni, L., Feo, L., Quattrini, A.*, et al.* (2020). Retromer stabilization results in neuroprotection in a model of Amyotrophic Lateral Sclerosis. Nat Commun *11*, 3848.

Ouellette, S.P., and Carabeo, R.A. (2010). A Functional Slow Recycling Pathway of Transferrin is Required for Growth of Chlamydia. Front Microbiol *1*, 112.
Pottier, C., Hannequin, D., Coutant, S., Rovelet-Lecrux, A., Wallon, D., Rousseau, S., Legallic, S., Paquet, C., Bombois, S., Pariente, J.*, et al.* (2012). High frequency of potentially pathogenic SORL1 mutations in autosomal dominant early-onset Alzheimer disease. Molecular psychiatry *17*, 875-879.
Rogaeva, E., Meng, Y., Lee, J.H., Gu, Y., Kawarai, T., Zou, F., Katayama, T., Baldwin, C.T., Cheng, R., Hasegawa, H.*, et al.* (2007). The neuronal sortilin-related receptor SORL1 is genetically associated with Alzheimer disease. Nat Genet *39*, 168-177.
Scheltens, P., De Strooper, B., Kivipelto, M., Holstege, H., Chetelat, G., Teunissen, C.E., Cummings, J., and van der Flier, W.M. (2021). Alzheimer's disease. Lancet *397*, 1577-1590.
Shi, Y., Kirwan, P., Smith, J., Robinson, H.P., and Livesey, F.J. (2012). Human cerebral cortex development from pluripotent stem cells to functional excitatory synapses. Nat Neurosci *15*, 477-486, S471.
Simoes, S., Guo, J., Buitrago, L., Qureshi, Y.H., Feng, X., Kothiya, M., Cortes, E., Patel, V., Kannan, S., Kim, Y.H.*, et al.* (2021). Alzheimer's vulnerable brain region relies on a distinct retromer core dedicated to endosomal recycling. Cell Rep *37*, 110182.
Sonnichsen, B., De Renzis, S., Nielsen, E., Rietdorf, J., and Zerial, M. (2000). Distinct membrane domains on endosomes in the recycling pathway visualized by multicolor imaging of Rab4, Rab5, and Rab11. J Cell Biol *149*, 901-914.
Tan, J.Z.A., and Gleeson, P.A. (2019). The role of membrane trafficking in the processing of amyloid precursor protein and production of amyloid peptides in Alzheimer's disease. Biochim Biophys Acta Biomembr *1861*, 697-712.
Tang, M., Harrison, J., Deaton, C.A., and Johnson, G.V.W. (2019). Tau Clearance Mechanisms. Adv Exp Med Biol *1184*, 57-68.
Toh, W.H., Chia, P.Z.C., Hossain, M.I., and Gleeson, P.A. (2018). GGA1 regulates signal-dependent sorting of BACE1 to recycling endosomes, which moderates Abeta production. Mol Biol Cell *29*, 191-208.
Vagnozzi, A.N., Li, J.G., Chiu, J., Razmpour, R., Warfield, R., Ramirez, S.H., and Pratico, D. (2021). VPS35 regulates tau phosphorylation and neuropathology in tauopathy. Molecular psychiatry *26*, 6992-7005.
Vardarajan, B.N., Zhang, Y., Lee, J.H., Cheng, R., Bohm, C., Ghani, M., Reitz, C., Reyes-Dumeyer, D., Shen, Y., Rogaeva, E.*, et al.* (2014). Coding mutations in SORL1 and Alzheimer's disease. Annals of neurology.
Young, J.E., Boulanger-Weill, J., Williams, D.A., Woodruff, G., Buen, F., Revilla, A.C., Herrera, C., Israel, M.A., Yuan, S.H., Edland, S.D.*, et al.* (2015). Elucidating Molecular Phenotypes Caused by the SORL1 Alzheimer's Disease Genetic Risk Factor Using Human Induced Pluripotent Stem Cells. Cell stem cell *16*, 373-385.
Young, J.E., Fong, L.K., Frankowski, H., Petsko, G.A., Small, S.A., and Goldstein, L.S.B. (2018). Stabilizing the Retromer Complex in a Human Stem Cell Model of Alzheimer's Disease Reduces TAU Phosphorylation Independently of Amyloid Precursor Protein. Stem Cell Reports *10*, 1046-1058.

Figure 1

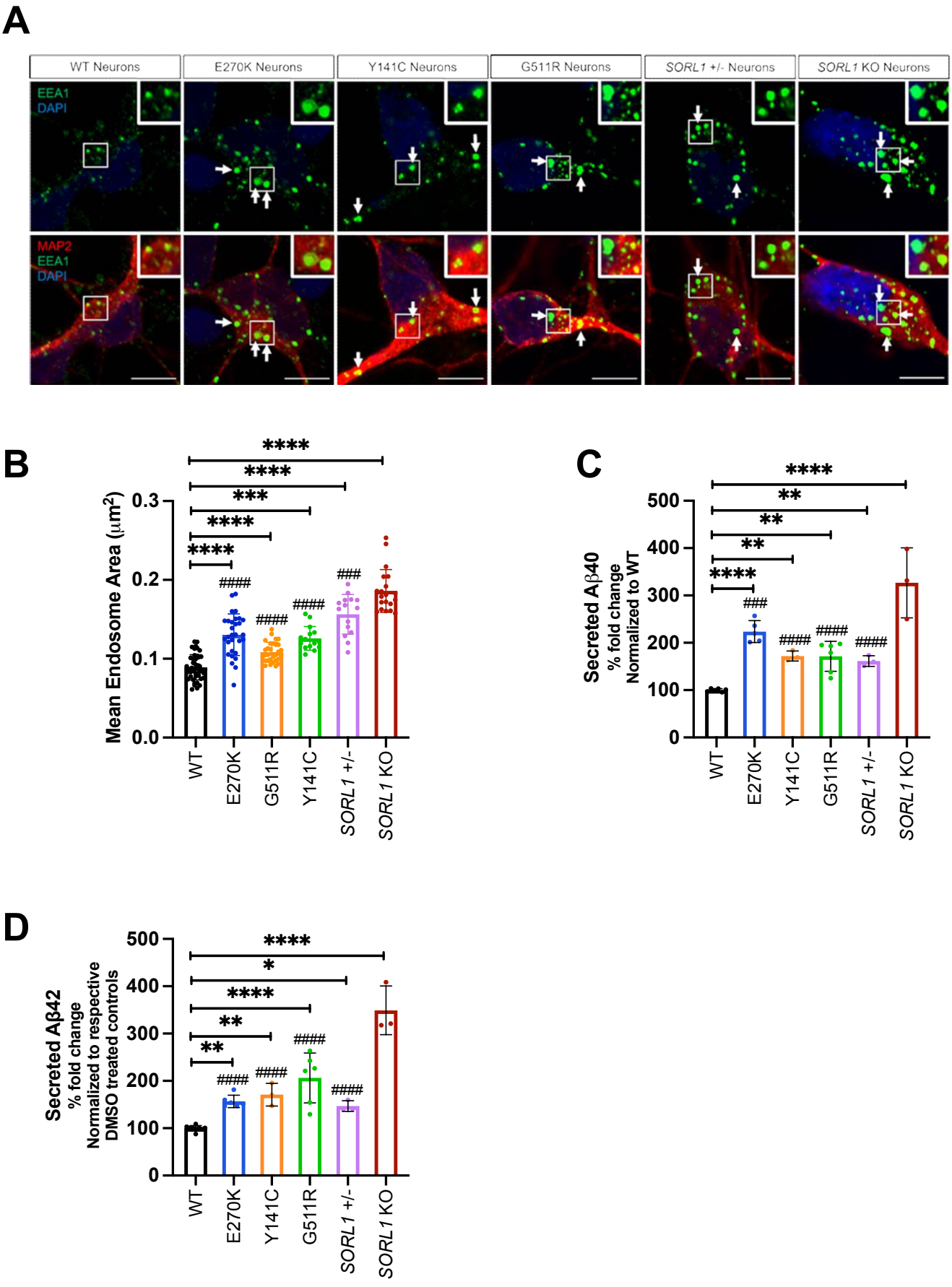
A
WT Neurons
E270K Neurons
Y141C Neurons
G511R Neurons
SORL1 +/- Neurons
SORL1 KO Neurons
EEA1
DAPI
MAP2
EEA1
DAPI
B
Mean Endosome Area (μm²)
0.0
0.1
0.2
0.3
****
****
***
****
****
####
####
####
####
###
WT
E270K
G511R
Y141C
SORL1 +/-
SORL1 KO
C
Secreted Aβ40
% fold change
Normalized to WT
0
100
200
300
400
500
****
**
**
**
****
###
####
####
####
WT
E270K
Y141C
G511R
SORL1 +/-
SORL1 KO
D
Secreted Aβ42
% fold change
Normalized to respective
DMSO treated controls
0
100
200
300
400
500
****
*
****
**
**
####
####
####
####
WT
E270K
Y141C
G511R
SORL1 +/-
SORL1 KO

Figure 2

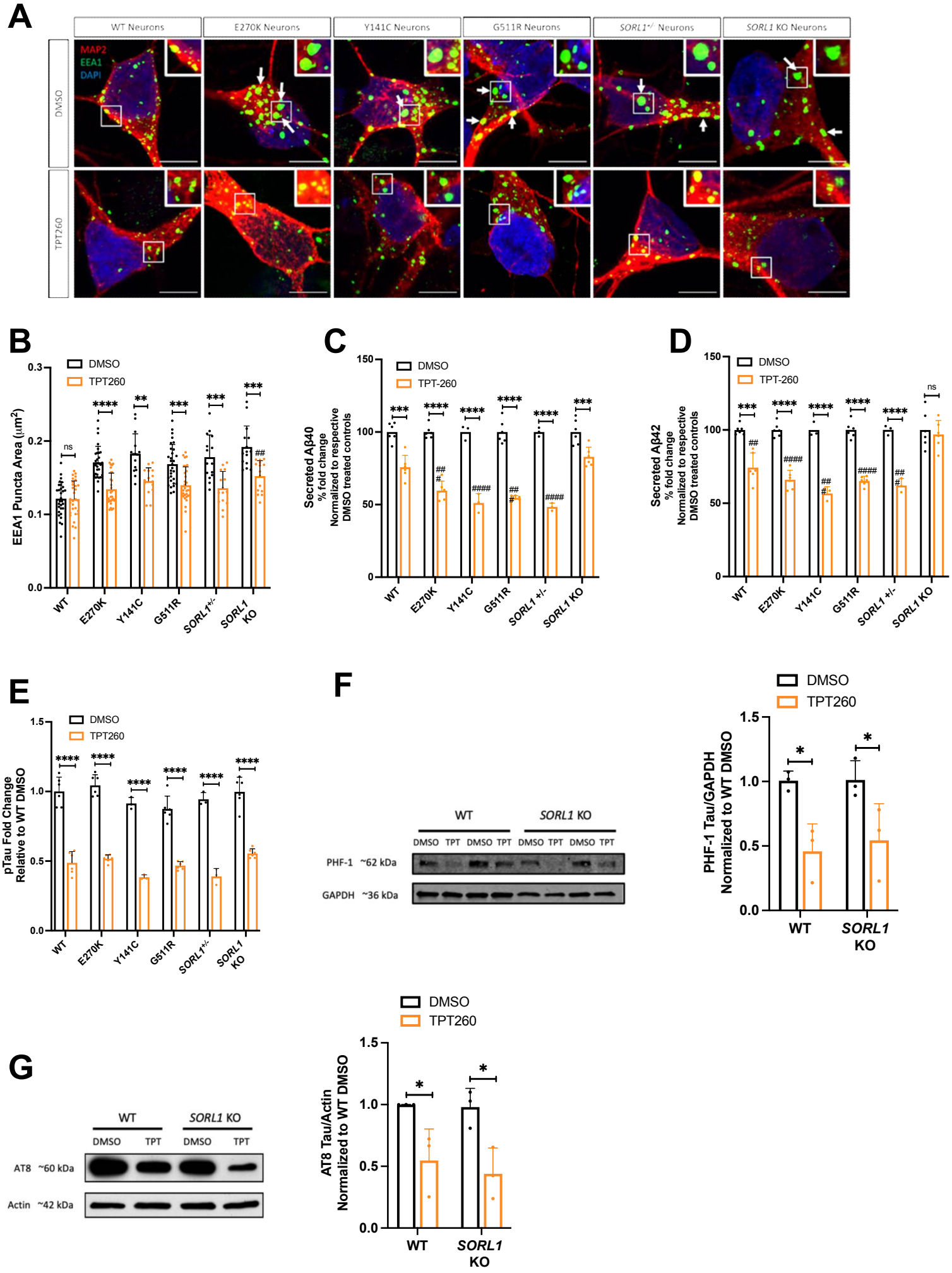

Figure 3

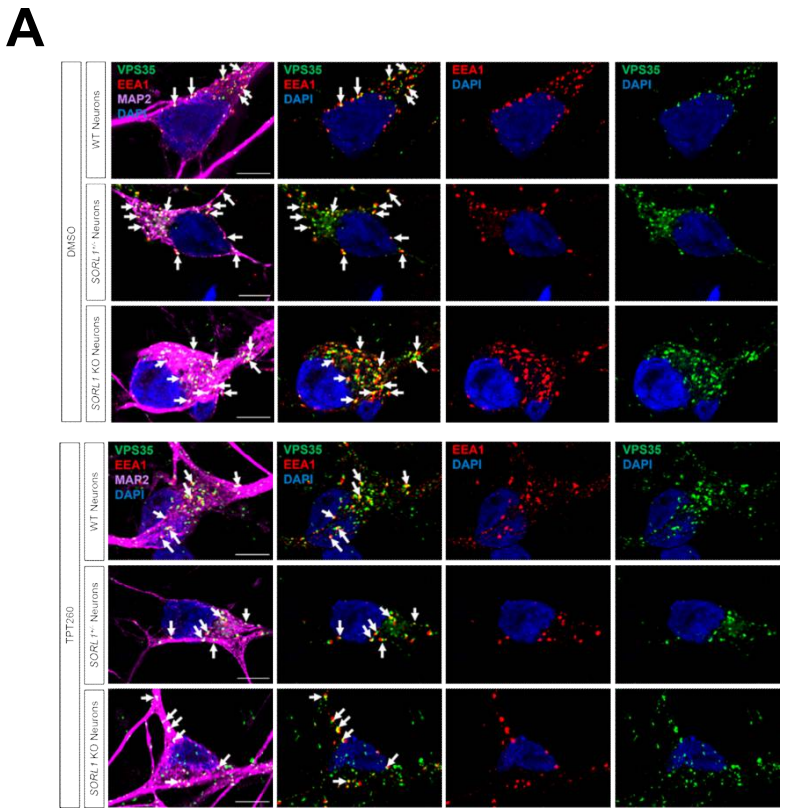
A
DMSO
TPT260
WT Neurons
SORL1+/- Neurons
SORL1 KO Neurons
VPS35
EEA1
MAP2
MAR2
DAPI

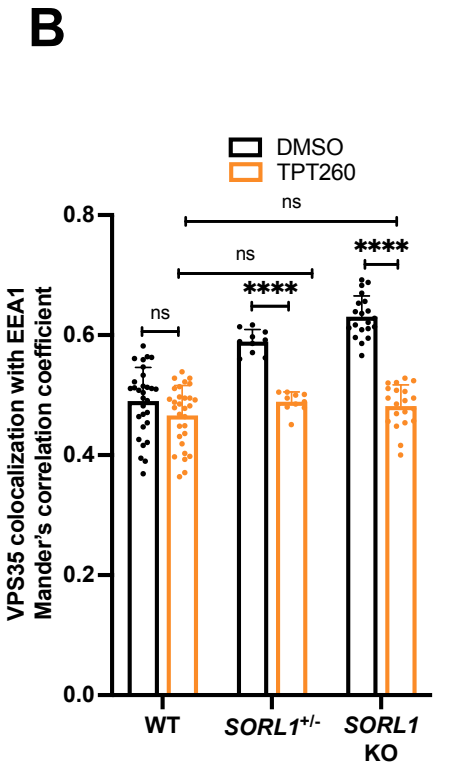
B
DMSO
TPT260
VPS35 colocalization with EEA1
Mander's correlation coefficient
0.0
0.2
0.4
0.6
0.8
ns
****
WT
SORL1+/-
SORL1
KO

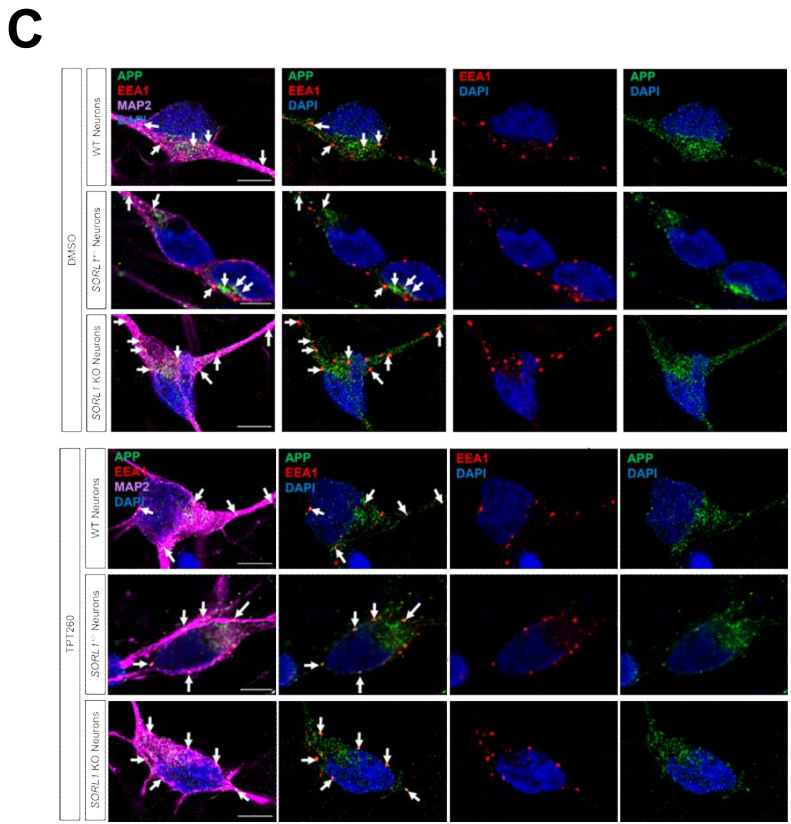
C
DMSO
TPT260
WT Neurons
SORL1+/- Neurons
SORL1 KO Neurons
APP
EEA1
MAP2
DAPI

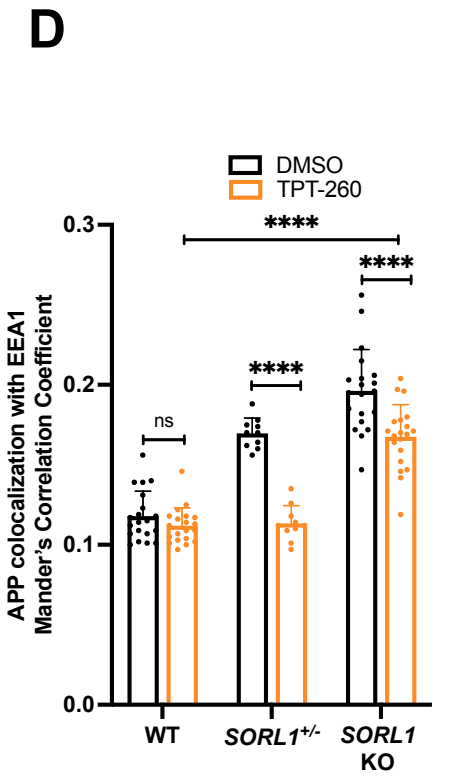
D
DMSO
TPT-260
APP colocalization with EEA1
Mander's Correlation Coefficient
0.0
0.1
0.2
0.3
ns
****
WT
SORL1+/-
SORL1
KO

Figure 4

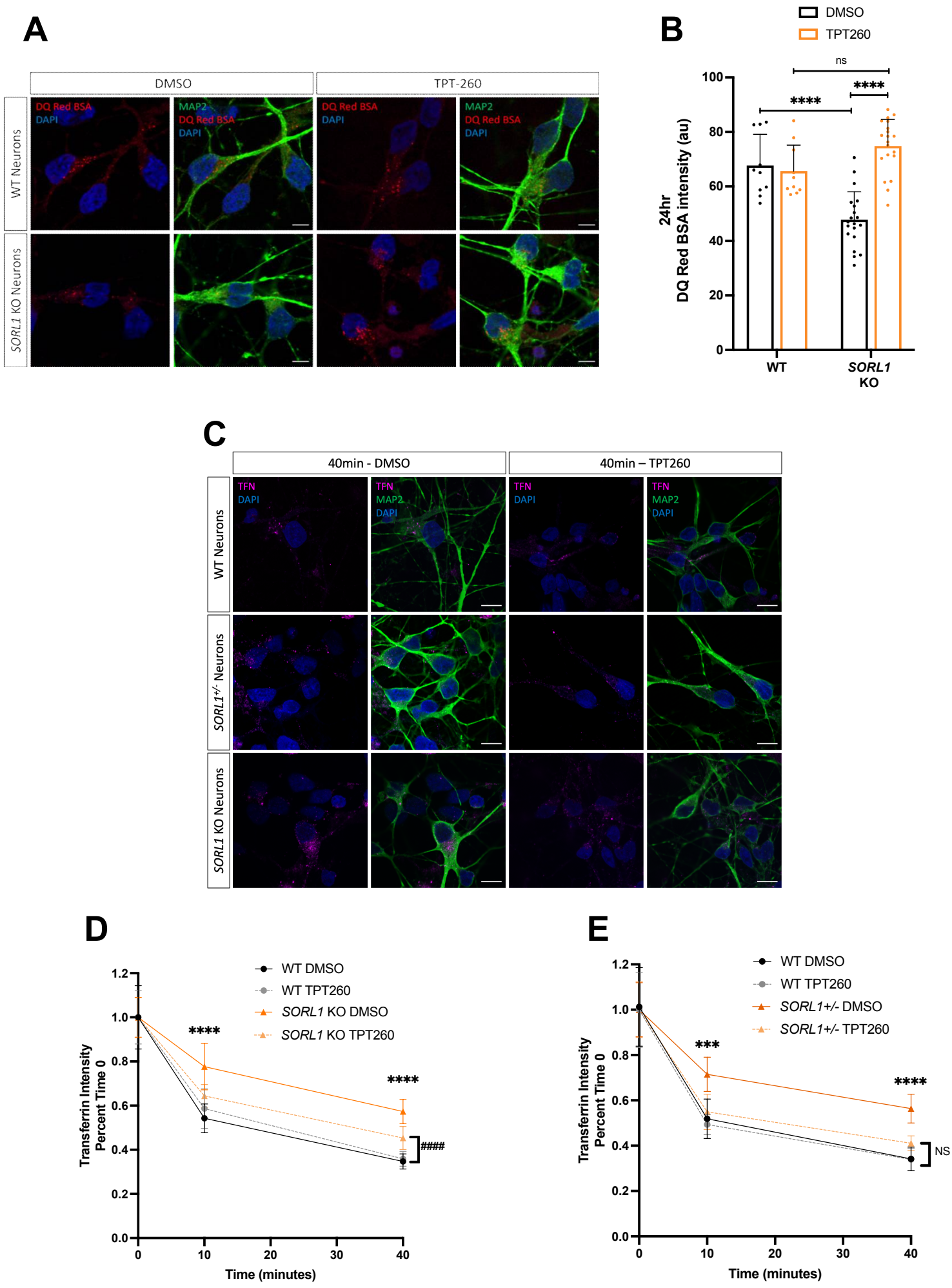

## Supplemental Figures

Supplemental Figure 1

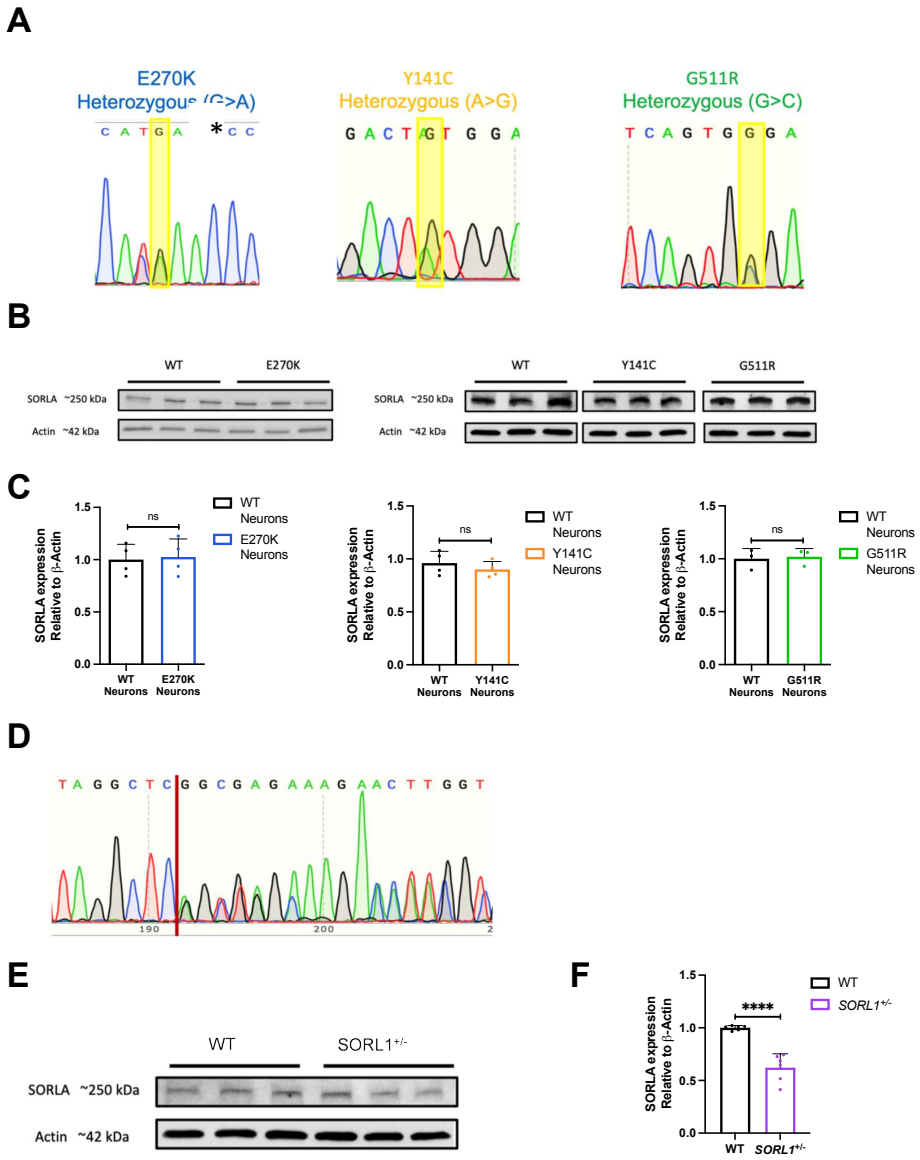


**Figure S1. Characterization of *SORL1*$^{Var}$ and *SORL1*$^{+/-}$ cell lines.**
**A)** Sanger sequencing showing heterozygous base-pair change for each *SORL1*$^{Var}$ hiPSC line. * indicates a synonymous SNP that is present in the genetic background of this hiPSC line. The E270K edit (G to A) is highlighted next to this SNP. **B)** Representative Western blots showing that *SORL1*$^{Var}$ hiPSCs have equivalent levels of SORLA protein expression to WT. **C)** Quantification of Western blots; E270K analysis: 2 WT and 2 E270K clones, 2 independent replicates per clone;Y141C analysis: 2 WT clones and 1 Y141C clone, 2 independent replicates per clone for WT and 4 independent replicates per clone for Y141C; G511R analysis: 1 WT clone, 3 independent replicates per clone. 1 G511R clone, 3 independent replicates per clone. **D)** Sanger sequencing showing heterozygous insertion/deletion (indel) leading to *SORL1*$^{+/-}$ hiPSC line. **E)** Representative Western blots showing that *SORL1*$^{+/-}$ hiPSCs have less SORLA protein expression

than WT hiPSCs. **F)** Quantification of Western blots; *SORL1*$^{+/-}$ analysis: 2 WT clones, 3 independent replicates per clone. 1 *SORL1*$^{+/-}$ clone, 6 independent replicates per clone.

Supplemental Figure 2

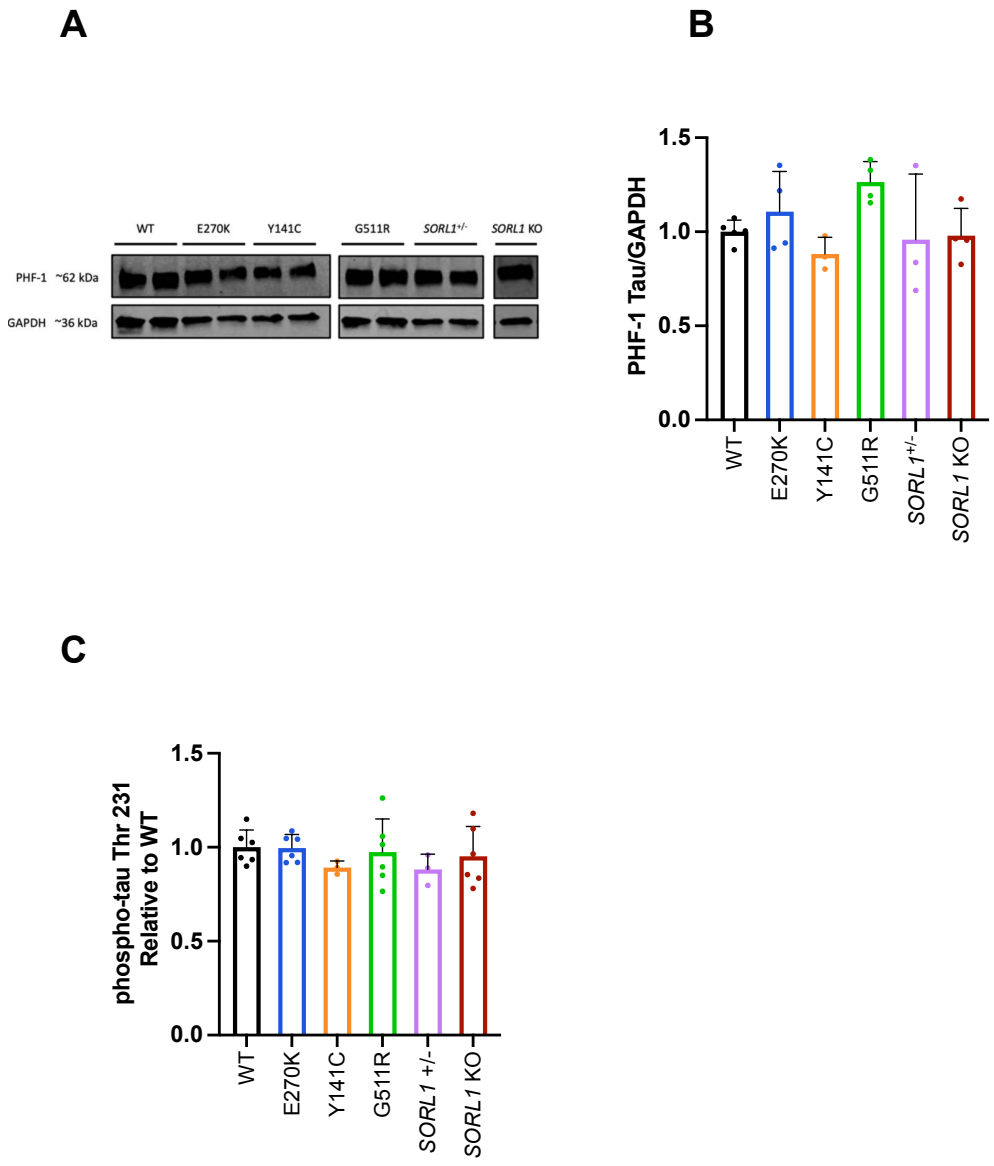


**Figure S2. Phospho-tau levels in *SORL1*KO, *SORL1*$^{Var}$ and *SORL1*$^{+/-}$ neurons. Related to Figure 2.** **A-C)** No significant change in phospho-tau at two epitopes was detected in *SORL1* KO, *SORL1*$^{Var}$, or *SORL1*$^{+/-}$ neurons. **A)** Representative Western blot of PHF-1 phospho-tau epitope. **B)** Quantification of Western blot; WT - 2 clones, 2 independent replicates for clone 1 (A7) and 3 independent replicates for

clone 2 (A6); E270K : 2 clones, 2 independent replicates per clone; Y141C : 1 clone, 3 independent replicates per clone; G511R : 2 clones, 2 independent replicates per clone; *SORL1*$^{+/-}$ : 1 clone, 3 independent replicates per clone; *SORL1* KO : 2 clones, 2 independent replicates per clone

**C)** ELISA assay of Thr 231 phospho-Tau epitope; WT : 2 clones, 3 independent replicates per clone; E270K: 2 clones, 3 independent replicates per clone; Y141C : 1 clone, 3 independent replicates per clone
G511R: 2 clones, 3 independent replicates per clone; *SORL1*$^{+/-}$: 1 clone, 3 independent replicates per clone; *SORL1* KO : 2 clones, 3 independent replicates per clone

**Table S1. Key Resources Table (related to experimental procedures and supplemental experimental procedures)**

| REAGENT or RESOURCE | SOURCE | IDENTIFIER |
|---|---|---|
| Antibodies | | |
| Rabbit monoclonal anti-SORLA | Abcam | Cat#ab190684 |
| Rabbit monoclonal anti-APP (clone Y188) | Abcam | Cat#ab32136; RRID: AB_2289606 |
| Mouse monoclonal anti-EEA1 | BD Biosciences | Cat#610456; RRID: AB_397829 |
| Rabbit polyclonal anti-VPS35 | Abcam | Cat#ab97545; RRID: AB_10696107 |
| Mouse monoclonal anti-Actin (clone AC-15) | Millipore Sigma | Cat#A5441; RRID: AB_476744 |
| Mouse monoclonal anti-Phospho-Tau (AT8) | Thermo Fisher Scientific | Cat#MN1020; RRID: AB_223647 |
| Rabbit monoclonal anti-GAPDH (14C10) | Cell Signaling | Cat#2118; RRID: AB_561053 |
| Chicken polyclonal anti-MAP2 | Abcam | Cat#92434; RRID:AB_2138147 |
| PHF-TAU antibody | Gift from Dr. Peter Davies | non-commercial antibody |
| Chemicals, peptides, and recombinant proteins | | |
| TPT-260 (hydrochloride) | Cayman Chemical | Cat#16079 |
| DQ-BSA | Thermo Fisher Scientific | Cat#D12051 |
| Critical commercial assays | | |
| Amyloid-beta V-PLEX Panel ELISA | Meso Scale Discovery | Cat#K15200E-2 |
| MULTI-SPOT Phospho (Thr231)/total tau assay | Meso Scale Discovery | Cat#K15121D-2 |
| Experimental models: Cell lines | | |
| Human Wildtype clone A6 iPSC cell line | Knupp et al 2020 | N/A |
| Human Wildtype clone A7 iPSC cell line | Knupp et al 2020 | N/A |
| Human *SORL1* Knockout clone E4 iPS cell line | Knupp et al 2020 | N/A |
| Human *SORL1* Knockout clone E1 iPS cell line | Knupp et al 2020 | N/A |
| Human *SORL1* variant E270K SORL1$^{Var}$ iPS cell line (2 clones) | This paper | N/A |
| Human *SORL1* variant G511R SORL1$^{Var}$ iPS cell line (2 clones) | This paper | N/A |
| Human *SORL1* variant Y141C SORL1$^{Var}$ iPS cell line (1 clone) | This paper | N/A |
| Human *SORL1* heterozygous SORL1$^{+/-}$ iPS cell line (1 clone) | This paper | N/A |
| Oligonucleotides | | |
| E270K SORL1$^{Var}$ gRNA targeting sequence: ATTGAACGACATGAACCCTC | Knupp et al 2020 | N/A |

| | | |
|---|---|---|
| E270K SORL1$^{Var}$ ssODN GGGAATTGATCCCTATGACAAACCAAATACCATCTAC ATTGAACGACATGAACCCTCTGGCTACTCCACGTCTT CCGAAGTACAGATTTCTTCCAGTCCCGGGAAAACCAG GAAG | Knupp et al 2020r | N/A |
| E270K *SORL1*$^{Var}$ Forward primer: ctctatcctgagtcaaggagtaac | Knupp et al 2020r | N/A |
| E270K *SORL1*$^{Var}$ Reverse primer: ccttccaattcctgtgtatgc | Knupp et al 2020 | N/A |
| Y141C *SORL1*$^{Var}$ gRNA targeting sequence: GTACGTGTCTTACGACTA | This paper | N/A |
| Y141C *SORL1*$^{Var}$ ssODN: GAAAGATCTTTCTGCCAGTTTCTCACCAACTCTTTCTT TTTCATCTCCTTTTCTCTGTATTCCAGGTGTACGTGTC TTACGACTGTGGAAAATCATTCAAGAAAATTTCAGACA AGTTAAACTTTGGCTTGGGAAATAGGAGTGAAGCTG | This paper | N/A |
| Y141C *SORL1*$^{Var}$ Forward primer: gtggcaggtgcctgtaatcc | This paper | N/A |
| Y141C *SORL1*$^{Var}$ Reverse primer: cacagagagcgccatctcc | This paper | N/A |
| G511R *SORL1*$^{Var}$ and SORL1$^{+/-}$gRNA targeting sequence: CTCTTGCATTTTAGGCTCAG | This paper | N/A |
| G511R *SORL1*$^{Var}$ ssODN: CTGACATATTCTTGAAATTAAAAATAATTATTTCTCTTG CATTTTAGGCTCAGTGCGAAAGAACTTGGCTAGCAAG ACAAACGTGTACATCTCTAGCAGTGCTGGAGCCAGG TGGCG | This paper | N/A |
| G511R *SORL1*$^{Var}$ Forward primer: cgccactggtaagtgtgcttgc | This paper | N/A |
| G511R *SORL1*$^{Var}$ Reverse primer: ctggcattactggtctctgccatg | This paper | N/A |
| *SORL1* gRNA targeting sequence: ATTGAACGACATGAACCCTC | Knupp et al 2020 | |

| | | |
|---|---|---|
| *SORL1* ssODN:<br>GGGAATTGATCCCTATGACAAACCAAATA<br>CCATCTACATTGAACGACATGAACCCTCTGGCTACTC<br>CACGTCTTCCGAAGTACAGATTTCTTCCAGTCCCGGG<br>AAAACCAGGAAG | Knupp et al 2020 | |
| *SORL1*: Forward primer ctctatcctgagtcaaggagtaac | Knupp et al 2020 | |
| *SORL1*: Reverse primer ccttccaattcctgtgtatgc | Knupp et al 2020 | |
| | | |
| Software and algorithms | | |
| CellProfiler | McQuin et al 2018 | https://cellprofiler.org/ |
| ImageJ/FIJI | Schindelin et al 2012 | https://imagej.nih.gov/ij/ |
| JACOP plugin | Bolte and Cordelieres et al 2006 | https://imagejdocu.tudor.lu/_media/plugin/analysis/jacop_2.0/just_another_colocalization_plugin/jacop_.jar |

## Supplemental Experimental Procedures

### Cell lines (CRISPR/Cas9 Genome Editing)

The Zhang Lab CRISPR Design website (crispr.mit.edu) was used to generate guide RNAs (gRNAs) with minimal off-target effects. gRNAs were cloned into the px458 vector that also expresses GFP and the Cas-9 nuclease. hiPSCs were electroporated with plasmids, sorted by flow cytometry for GFP expression, and plated at a clonal density of ~1x10^4 cells per 10cm plate. After approximately two weeks of growth, colonies were picked and split into identical sets. Further details of the cell lines are described in the supplemental experimental procedures, and Tables S1. One set was analyzed by Sanger sequencing and one set was expanded to generate isogenic cell lines.

A total of 8 previously unpublished clones were chosen for experiments contained in this publication: 2 WT clones, 2 clones containing the heterozygous *SORL1* E270K variant (Figure S1), 1 clone containing the heterozygous *SORL1* Y141C variant (Figure S1), 2 clones containing the heterozygous *SORL1* G511R variant (Figure S1), and 1 clone containing a deletion resulting in a heterozygous *SORL1* KO (*SORL1* $^{+/-}$ ) (Figure S2). Also included in this publication are four previously published clones including 2 WT clones and 2 homozygous *SORL1* KO clones (*SORL1* KO)(1, 2). All clones were shown to have normal karyotypes and verified to be free of mycoplasma (MycoAlert).

### CRISPR/Cas9 gRNA, ssODN, and Primer Sequences

The CRISPR/Cas9 reagents used to generate the E270K cell lines are the same as what was used to generate the previously published *SORL1* KO hiPSC lines(1). For the *SORL1* KO lines, clones were chosen that incorporated indels rather than the ssODN sequence.

E270K gRNA: ATTGAACGACATGAACCCTC
E270K ssODN:
GGGAATTGATCCCTATGACAAACCAAATACCATCTACATTGAACGACATGAACCCTCTGGCTACTCCA
CGTCTTCCGAAGTACAGATTTCTTCCAGTCCCGGGAAAACCAGGAAG
E270K Forward primer: ctctatcctgagtcaaggagtaac
E270K Reverse primer: ccttccaattcctgtgtatgc
PCR amplifies 458 bp sequence

Y141C gRNA: GTACGTGTCTTACGACTA
Y141C ssODN:
GAAAGATCTTTCTGCCAGTTTCTCACCAACTCTTTCTTTTTCATCTCCTTTTCTCTGTATTCCAGGTGT
ACGTGTCTTACGACTGTGGAAAATCATTCAAGAAAATTTCAGACAAGTTAAACTTTGGCTTGGGAAAT
AGGAGTGAAGCTG
Y141C Forward primer: gtggcaggtgcctgtaatcc
Y141C Reverse primer: cacagagagcgccatctcc
PCR amplifies 445 bp sequence

G511R gRNA: CTCTTGCATTTTAGGCTCAG
G511R ssODN:
CTGACATATTCTTGAAATTAAAAATAATTATTTCTCTTGCATTTTAGGCTCAGTGCGAAAGAACTTGGC
TAGCAAGACAAACGTGTACATCTCTAGCAGTGCTGGAGCCAGGTGGCG
G511R Forward primer: cgccactggtaagtgtgcttgc
G511R Reverse primer: ctggcattactggtctctgccatg
PCR amplifies 413 bp sequence

*SORL1*$^{+/-}$: The *SORL1*$^{+/-}$ line was generated with the same gRNA as the *SORL1* G511R line. The PCR primers and amplicon are the same as for G511R.

### Neuronal Differentiation

Cortical neurons were differentiated from hiPSCs using the dual-SMAD inhibition technique. hiPSCs were plated on 1:20 Matrigel-coated (Growth factor reduced basement membrane matrix; # 356231; Corning) 6-

well plates at a density of 3.5 million cells per well. Cells were fed with Basal Neural Maintenance Media (BNMM) (1:1 DMEM/F12 (#11039047 Life Technologies) + glutamine media/neurobasal media (#21103049, Gibco), 0.5% N2 supplement (# 17502-048; Thermo Fisher Scientific,) 1% B27 supplement (# 17504-044; Thermo Fisher Scientific), 0.5% GlutaMax (# 35050061; Thermo Fisher Scientific), 0.5% insulin-transferrin-selenium (#41400045; Thermo Fisher Scientific), 0.5% NEAA (# 11140050; Thermo Fisher Scientific), 0.2% β-mercaptoethanol (#21985023, Life Technologies)) supplemented with 10 μM SB-431542 and 0.5 μM LDN-193189 (#1062443, Biogems) for seven days. On day 8, cells were incubated with Versene (#15640066, Gibco), dissociated with cell scrapers, and passaged 1:3. From days 9-13, cells were fed daily with BNMM containing no supplements. On day 13, media was switched to BNMM containing 20 ng/mL FGF (R&D Systems, Minneapolis, MN). On day 16, cells were passaged 1:3. Cells were fed daily until approximately day 23, when cells were FACS sorted to enrich a stable population of CD184/CD24 (#557145/561646 BD Pharmingen) positive, CD44/CD271 (#555479/557196 BD Pharmingen) negative neural progenitor cells(3). After sorting, cells were expanded for cortical neuronal differentiation. Neural progenitor cells were plated on Matrigel at a density of 5 million cells per 10cm plate. Media was switched to BNMM supplemented with 0.02 μg/mL brain-derived neurotrophic factor (#450-02 PeproTech) + 0.02 μg/mL glial-cell-derived neurotrophic factor (#450-10 PeproTech) + 0.5 mM dbcAMP (#D0260 Sigma Aldrich). Cells were fed twice a week for three weeks. After three weeks, neurons were sorted by magnetic activated techniques to enrich the population of CD184/CD44/CD271 negative cells and plated out for experiments. All cell culture was maintained at 37C and 5% $CO_2$.

**Purification of hiPSC-derived neurons**

Following 3 weeks of differentiation, neurons were dissociated with accutase and resuspended in Magnet Activated Cell Sorting (MACS) buffer (PBS + 0.5% bovine serum albumin [Sigma Aldrich, St Louis, MO] + 2 mM ethylenediaminetetraacetic acid [Thermo Fisher Scientific, Waltham, MA]). Following a modification of(3) cells were incubated with PE-conjugated mouse anti-Human CD44 and mouse anti-Human CD184 antibodies (BD Biosciences, San Jose, CA) at a concentration of 5 μl/10 million cells. Following antibody incubation, cells were washed with MACS buffer and incubated with anti-PE magnetic beads (BD Biosciences, San Jose, CA) at a concentration of 25 μl/10 million cells. Bead-antibody complexes were pulled down using a rare-earth magnet, supernatants were selected, washed, and plated at an appropriate density.

**DQ Red BSA assay**

Lysosomal proteolytic degradation was evaluated using DQ Red BSA (#D-12051; Thermo Fisher Scientific), a fluorogenic substrate for lysosomal proteases, that generates fluorescence only when enzymatically cleaved in intracellular lysosomal compartments. hiPSC-derived neurons were seeded at a density of 400,000 cells/well of a Matrigel coated 48-well plate. After 24 h, cells were washed once with DPBS, treated with complete media containing either 10 μg/ml DQ Red BSA or vehicle (PBS) and incubated for 24 h at 37 °C in a 5% CO2 incubator as described in(4) and(5). At the end of 24 h, cells were washed with PBS, fixed with 4% PFA and immunocytochemistry was performed as described below in Supplemental Experimental Procedures. Cells were imaged using a Leica SP8 confocal microscope and all image processing was completed with ImageJ software. Cell bodies were identified by MAP2 labeling, and fluorescence intensity of DQ Red BSA was measured in regions of the images containing the MAP2 label.

**Transferrin recycling assay**

Purified neurons were seeded at 400,000 cells/well of a 24-well plate containing Matrigel coated 12 mm glass coverslips/well. After 5 DIV, cells were washed once with DMEM-F12 medium and incubated with starving medium (DMEM-F12 medium + 25 mM HEPES + 0.5% BSA) for 30 min at 37 °C in a 5% CO2 incubator to remove any residual transferrin. Thereafter, cells were pulsed with either 100 μg/ml transferrin from human serum conjugated with Alexa Fluor™ 647(#T23366; Thermo Fisher Scientific) or vehicle (PBS) in 'starving medium'. At the end of 10 min, cells were washed twice with ice-cold PBS to remove any external transferrin and stop internalization of transferrin and washed once with acid stripping buffer (25 mM citric acid + 24.5 mM sodium citrate + 280 mM sucrose + 0.01 mM Deferoxamine) to remove any

membrane bound transferrin. Next, cells were either fixed in 4% PFA or 'Chase medium' (DMEM-F12 + 50 µM Deferoxamine + 20 mM HEPES + 500 µg/ml Holo-transferrin) was added for different time points. Immunocytochemistry was done using MAP2 antibody to label neurons, confocal images were captured using Leica SP8 confocal microscope under blinded conditions. Fluorescence intensity of transferrin was measured using ImageJ software.

**Western blotting**

Cell lysates were run on 4%–20% Mini-PROTEAN TGX Precast Protein Gels (#4561096; Biorad) or 16.5% Criterion Tris-Tricine Gel (#3450063; BioRad) and transferred to PVDF membranes. Membranes were probed with antibodies described in the Key resources table. Imaging was performed with a BioRad ChemiDoc system and quantification was performed using ImageJ software. For Western blot analysis, hiPSC-neurons were washed with PBS and harvested in RIPA buffer containing 1X protease and 1X phosphatase inhibitors. Total protein concentration was quantified using Pierce BCA assay kit (#23225; Thermo Fisher Scientific). Cell lysates were separated on a 4-20% Mini-PROTEAN TGX Precast Protein Gels (#4561096; Biorad). Proteins were then transferred to PVDF membranes and membranes were incubated with antibodies to Sortilin-related receptor 1 (SORLA) at 1:1000 (# ab190684; abcam); Mouse monoclonal anti-Actin (clone A4) (#MAB1501; Millipore Sigma) at 1:2000; Mouse monoclonal anti-Phospho-Tau (AT8) (#MN1020; Thermo Fisher Scientific) and Rabbit monoclonal anti-GAPDH (14C10) (#2118; Cell Signaling) and Rabbit polyclonal anti-VPS35 ( #ab97545; Abcam) at 1:1000. For the PHF-Tau blots, blots were incubated overnight with PHF-1, Gift from Dr. Peter Davies, mouse 1:1000. After three washes with TBST, membranes were incubated with corresponding IRDye fluorescent secondary antibodies in intercept blocking buffer (Li-Cor) for 1h and scanned using an Odyssey Clx imaging system (Li-Cor).

**Immunocytochemistry**

Purified neurons were seeded at a density of 500,000 cells per well of a 24-well plate on glass coverslips coated with Matrigel. After 5 days in culture, cells were fixed in 4% paraformaldehyde (PFA, Alfa Aesar, Reston, VA) for 15 minutes. Cells were incubated in blocking buffer containing 2.5% bovine serum albumin and 0.1% Triton X-100 (Sigma Aldrich, St Louis, MO) for 30 minutes at room temperature then incubated in a primary antibody dilution in blocking buffer for 2 hours at room temperature. Cells were washed 3x with PBS + 0.1% Triton X-100 and incubated with a secondary antibody dilution in blocking buffer for 1 hour at room temperature. Cells were washed 3x in PBS and mounted on glass slides with ProLong Gold Antifade mountant (#P36930; Thermo Fisher Scientific, Waltham, MA). For details of antibodies used, see table S1.

**Confocal microscopy and Image processing**

Confocal z stacks were obtained using a Nikon A1R confocal microscope with x63 and x100 plan apochromat oil immersion objectives or a Yokogawa W1 spinning disk confocal microscope (Nikon) and a 100X plan apochromat oil immersion objective. Maximum intensity projections of confocal stacks were generated, and background was subtracted using the rolling ball algorithm. Endosome channels were enhanced using contrast limited adaptive histogram equalization algorithms (CLAHE) and masked using cell body stains. Size and intensity measurements were performed using Cell Profiler software(6). Individual puncta were identified using automated segmentation algorithms. Mean intensity of each puncta was measured and has been presented as a mean value over all puncta per field. Similarly, pixel area of each puncta was measured and has been presented as a mean area over all puncta per field. Finally, mean puncta area normalized by total cell area calculated from cell body stains is also presented

**Quantification and statistical analysis**

For early endosome size analysis, 3 clones of WT, 2 clones of E270K *SORL1*$^{var}$ , 1 clone of Y141C *SORL1*$^{var}$, 2 clones of G511R *SORL1*$^{var}$, 1 clone of *SORL1*$^{+/-}$ and 2 clones of *SORL1* KO were used. 10-15 images per clones were analyzed. For experiments measuring secreted Aβ, 3 clones of WT, 2 clones of E270K*SORL1*$^{var}$, 1 clones of Y141C *SORL1*$^{var}$, 2 clones of G511R *SORL1*$^{var}$, 1 clone of *SORL1*$^{+/-}$ and 1 clone of *SORL1* KO were used. 3 replicates per clone were analyzed for this experiment. For APP/EEA1 and VPS35/EEA1 colocalization experiments, 2 clones of WT, 2 clones of *SORL1* KO and 1 clone of *SORL1*$^{+/-}$ were used. 10 images per clone were analyzed for this experiment. For measurement of phosphorylated and total tau experiments, 2 clones of WT, 2 clones of E270K *SORL1*$^{var-}$, 1 clone of Y141C

*SORL1*$^{var}$ , 2 clones of G511R *SORL1*$^{var}$, 1 clone of *SORL1*$^{+/-}$ and 2 clones of *SORL1* KO were used. 3 replicates per clone were analyzed for this experiment. For detection of tau using western blotting, 2 clones of WT and 2 clones of *SORL1* KO were used. 1-2 replicates per clone per condition were analyzed for this experiment. For early endosome size analysis with TPT-260 treatment experiments, 2 clones of WT, 2 clones of E270K *SORL1*$^{var}$, 1 clone of Y141C *SORL1*$^{var}$, 2 clones of G511R *SORL1*$^{var}$, 1 clone of *SORL1*$^{+/-}$ and 1 clone of *SORL1* KO were used. 15 images per clone per condition were analyzed for this experiment. For DQ-BSA assay, 1 clone of WT and 2 clones of *SORL1* KO were used and 10 images per clone per time point per condition was analyzed. For transferrin recycling assay, 2 WT clones, 1 SORL1$^{+/-}$, and 2 *SORL1* KO clones were used and 10 images per clone per time point per condition were analyzed.

**Supplemental References**

1. Knupp A, Mishra S, Martinez R, Braggin JE, Szabo M, Kinoshita C, et al. Depletion of the AD Risk Gene SORL1 Selectively Impairs Neuronal Endosomal Traffic Independent of Amyloidogenic APP Processing. Cell Rep. 2020;31(9):107719.
2. Mishra S, Knupp A, Szabo MP, Williams CA, Kinoshita C, Hailey DW, et al. The Alzheimer's gene SORL1 is a regulator of endosomal traffic and recycling in human neurons. Cell Mol Life Sci. 2022;79(3):162.
3. Yuan SH, Martin J, Elia J, Flippin J, Paramban RI, Hefferan MP, et al. Cell-surface marker signatures for the isolation of neural stem cells, glia and neurons derived from human pluripotent stem cells. PLoS One. 2011;6(3):e17540.
4. Marwaha R, Sharma M. DQ-Red BSA Trafficking Assay in Cultured Cells to Assess Cargo Delivery to Lysosomes. Bio Protoc. 2017;7(19).
5. Davis SE, Roth JR, Aljabi Q, Hakim AR, Savell KE, Day JJ, et al. Delivering progranulin to neuronal lysosomes protects against excitotoxicity. J Biol Chem. 2021;297(3):100993.
6. McQuin C, Goodman A, Chernyshev V, Kamentsky L, Cimini BA, Karhohs KW, et al. CellProfiler 3.0: Next-generation image processing for biology. PLoS Biol. 2018;16(7):e2005970.